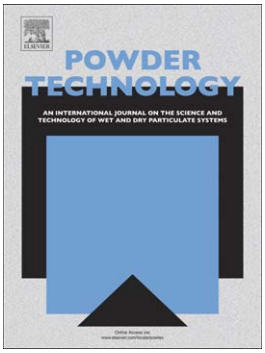

Three dimensional shape analysis of concrete aggregate fines produced by VSI crushing

Rolands Cepuritis, Edward J. Garboczi, Stefan Jacobsen

PII: S0032-5910(16)30884-1
DOI: doi:10.1016/j.powtec.2016.12.020
Reference: PTEC 12168

To appear in: *Powder Technology*

Received date: 5 July 2016
Revised date: 17 October 2016
Accepted date: 3 December 2016

Please cite this article as: Rolands Cepuritis, Edward J. Garboczi, Stefan Jacobsen, Three dimensional shape analysis of concrete aggregate fines produced by VSI crushing, *Powder Technology* (2016), doi:10.1016/j.powtec.2016.12.020

Three dimensional shape analysis of concrete aggregate fines produced by VSI crushing

Rolands Cepuritis [a,b,*], tel.: +47 95133075, rolands.cepuritis@norcem.no
Edward J. Garboczi [c], edward.garboczi@nist.gov
Stefan Jacobsen [a], stefan.jacobsen@ntnu.no

[a] Department of Structural Engineering, Norwegian University of Science and Technology, NO-7491 Trondheim, Norway
[b] Norcem AS (HeidelbergCement), R&D Department, Setreveien 2, Postboks 38, NO-3950 Brevik, Norway
[c] National Institute of Standards and Technology, Boulder, CO 80305, United States

Abstract: We studied the 3-D shape of concrete aggregate fines with particle sizes between 3 µm and 250 µm produced by high-speed vertical shaft impact (VSI) crushing of rock types from 10 different quarries representing a wide range of local Norwegian geology with respect to mineralogy and mechanical properties. This included igneous (intrusive and extrusive), metamorphic, and sedimentary rocks that were both mono- and multi-mineralic. VSI crushing seems to be able to generate concrete aggregate fines of very similar equidimensional mean shape characteristics for the whole analysed size range, independent of the mineralogical composition of the rocks included in the study. The effect on normalising the average particle shape was somewhat lower for the particle size range smaller than about 15 µm, where there seems to be a greater influence of the crystallographic structure of the individual minerals. Particles of the rock type containing the highest mica content (5.5 %, by mass) had the least equidimensional shape. The most equidimensional shape in a given particle size range was found for both limestone rock types that were analysed. A new shape parameter, the micro-Flakiness Index (µFI), has been proposed to characterize the shape of the fine crushed concrete aggregate particles to enable practical use of shape parameters.

Keywords: Crushed aggregate fines, VSI crusher, shape, Zingg's diagram, X-ray tomography, µFlakiness index.

1. INTRODUCTION

Vertical shaft impact (VSI) rock-on-rock crushing is a popular technique used for improving the average shape of crushed aggregate particles (making the particles more equi-axed), especially as part of the last comminution stage at hard rock quarries for production of high quality crushed sands [1], [2], [3], [4], [5], [6], [7]. The industries that make the most use of crushed rock and sand, the concrete and asphalt industries, tend to find the flow of their suspensions before hardening to be greatly influenced by particle shape, with more equi-axed particles giving easier flow characteristics. This is why the definition of "improving" the particle shape is used for describing the effect of VSI crushing. The advantage of the VSI crusher in sand production is that it produces equidimensional particles in most of the fraction sizes where particle shape is easily measurable by common "macro-scale" test methods, *i.e.* down to about 1 mm [8], [9], [10]. The disadvantage is that it produces larger amounts of fines[1] (also interchangeably referred to as filler or powder in this paper) than does the more common cone crusher technology [11], [12], [13], [14], because the dominant size reduction mechanism is inter-particle attrition and impact [11].

Typically the largest practical concern with respect to the application of crushed sand in concrete is the rheological performance in fresh mixes [3], [15], [16], [17], [18], [19], [20], [21], [22]. Studies with respect to the effect of different aggregate particle size groups on the rheology of fresh concrete suggest that particle shape characteristics matter more as particle size decreases [23], [24], [25]. VSI is known to change aspects of particle shape. To fully understand how VSI crushing does this, and the complete range of particle shape changes it can make, it would be necessary to understand the influence of all the variables involved in VSI crushing (*e.g.*, rotor speed, cascade flow, influence of a closed circuit, feed rock size and characteristics). In this

[1] The particle size definition of concrete aggregate fines is diverse. According to the European EN 12620 standard [95] fines are all material less than 63 µm. The US ASTM standard C33 / C33M – 13 [94] has a similar limit of 75 µm. For practical concrete purposes, it is, however, most common that all material less than 125 µm [76] or 250 µm [96] is referred to as fines.

paper, we only look at, for a given set of VSI variables, the effect of VSI crushing on the shape characteristics of aggregate particles smaller than 1 mm.

Since VSI crushing creates a considerable amount of fines, this process increases the smaller portions of the particle size range specified for a given application. Indeed, for practical applications of VSI crushers for production of crushed sand at hard rock quarries, it is of most interest to investigate the shape of the fines generated during the VSI crushing rather than those already existing in the feed material. This is because typically any fine particles are sieved out of the material fed to a VSI crusher and the feed fractions are mostly of the sizes of approx. 4/16 mm and 4/22 mm, *i.e.* the final crushed sand product includes only fines generated during the crushing process. The reasons for removing the fines from the VSI crusher feed when producing crushed sand typically include:

- desire to limit the total fines content in the VSI crushed sand product, so that the potential need to remove the excess of the total fines by, for example, washing or air-classification can be eliminated;
- desire to maximise the shaping of the coarser aggregate particles as fines in the VSI crusher feed create a kind of "cushion effect" reducing the impact energy at collision of the coarser aggregate particles.

In fact, as a great number of the fines in the final product are created during the VSI crushing process, experimentally, it is impossible to distinguish, in the same size range, between the fine particles created during the VSI crushing process and those that were part of the original feed material. Further, it would not be representative of the actual process to only process a feed of fines with the VSI crushing equipment. Thus the approach in this paper has been aimed at measuring the average shape of the new fines actually produced, rather than changes in the average shape of the powder particles in the specified particle size range.

A limited study of simple shape analysis of VSI processed crushed aggregate particles smaller than 1 mm has been performed by Bengtsson [26] and Bengtsson and Evertsson [11]. They have measured shape characteristics of sand particles crushed from tonalite rocks, which is an

igneous, intrusive rock, of felsic composition. The sand particles were produced using either a cone crusher or a VSI. The F-shape parameter is defined to be the ratio between the maximal and minimal Feret diameters x_{Fmax} and x_{Fmin}, which are defined by the maximum and minimum distance between parallel tangents in a 2-D particle image projection [27]. The x_{Fmax} and x_{Fmin} parameters are determined from analysis of 2-D images obtained by light microscope or scanning electron microscope (SEM) images, depending on the particle size, of polished sections of narrow particle fractions cast in epoxy. In these studies [26], [11], the VSI was run at three different rotor velocities, *i.e.* low (45 m/s), medium (60 m/s) and high (75 m/s). The results showed [26], [11] that the VSI rotor needs a minimum rotor velocity in order to significantly change the average particle shape compared to the cone crusher results. In this study, a higher rotor velocity led to increased fines content and more equidimensional particles in the sand particle size range of 0.063 mm to 4 mm. Bengtsson [26] and Bengtsson and Evertsson [11] also demonstrated that sand particle shape, produced with the medium cone crusher chamber set at a value of 20 mm for the Closed Side Setting (CSS) was much less equidimensional compared to that produced at high rotor speed (75 m/s) in a VSI . The CSS is the minimum distance between the liner (the inner part of the cone crusher) and the concave (the external part of the cone crusher) at the discharge end of the crushing cavity (the space between liner and concave where crushing action itself takes place).

In another study, Åkesson and Tjell [28] analysed the F-shape parameter of crushed aggregate fine particles in a size range of 0.036 mm to 1 mm, which were taken from eight different Swedish granite and gneiss rock types composed of various amounts of quartz, feldspar and mica. The analysed particles were produced by using particles of size between 4 mm and 8 mm to feed a VSI running at a rotor velocity of 60 m/s. The selection of materials for their study was based on varying the size of individual mineral crystals in the rock (micro to coarse grained) and mica content (2 % to 35 %, by volume). Their results showed that the VSI crusher had improved (in the sense defined above) the F-shape distribution and average of all the materials with particle size above 0.036 mm, except for one rock sample in the particle size range of 0.036 mm to 0.063 mm, compared to cone crushed powders using the same rock types. The rock type where there was no relative improvement in the 0.036 mm to 0.063 mm size range was the one with the highest mica content. From these results, Åkesson and Tjell [28] concluded that it may

be possible to improve the shape of single quartz and feldspar free mineral grains while the shape of a single mica grain may not be improved by the VSI. This was reinforced by the fact that the relative improvement of the shape could be related to the concentration of the mica in the parent rock.

The theoretical mechanism of impact comminution used by the VSI suggests that cleavage during crushing could be expected to take place in most solids over the plane of least surface energy, which are the individual mineral grain boundaries of the crushed rock materials [29]. This mechanism seems to form the foundation for the common opinion of aggregate and concrete production engineers regarding how the very fine aggregate particle shape will be affected during rock crushing. Lagerblad, et al. [30] have argued that, below a certain size, the particles from crushed rocks are mainly free mineral, the types of minerals depend on the rock type, and the mineral grain size of the rock determines the particle size when free minerals appear. Lagerblad, et al. [30] have also stated that at small particle sizes, the shape of the particle depends on the crystallographic structure of the individual mineral and the most troublesome minerals are those of the mica group as the crystal structure as such is quite layered. However, this statement has been only partly experimentally verified for the mentioned free mica particles, which are known to result from cleavage of thin layered sheets and are thought to be easily warped. This is why it is also believed that they might not be easy to crush, because the flaky sheets could deflect in the crushing chamber instead of being crushed, and their actual size and shape in the crusher product should then be similar to their mineral size and shape in the parent rock [31]. This has been partly confirmed experimentally by several researchers [32], [33], who have found that for some rock types it is indeed possible to observe a peak of the free mica content between 250 μm to 500 μm or 125 μm to 250 μm crushed filler sizes that corresponds to the approximate mineral size in the parent rock texture. It must, however, also be noted that enrichment in the free mica particles was also found for grains ≤ 63 μm [32], [33], and in fact some free mica grains were found also among the rest of the analysed particles. This suggests that some shaping of the mica particles is actually possible, as the chipped off pieces of the free mica particles probably end up in the ≤ 63 μm particle size group and cause the observed enrichment. In the reported studies [32], [33] no attempts to systematically study the shape of the free mica grains has been reported.

A new development within the last fifteen years is the use of X-ray computed tomography (CT), coupled with spherical harmonic (SH) analysis, to mathematically describe the full 3-D shape of particles and compute almost any geometrical property of the particles in 3-D [34], [35], [36], [37], [38], [39], [40], [41], [42], [43], [44], [45]. This technique has been successfully applied to obtain differentiable mathematical functions describing the actual 3-D shape of crushed rock aggregate powders as small as a Volume Equivalent Spherical Diameter (VESD) of 3 µm [45]. Performing 3-D shape analysis will avoid any 2-D artefacts, since image analysis only deals with 2-D projections of the particles.

This paper presents detailed studies of the 3-D shape of VSI crushed concrete aggregate fines from 10 different Norwegian rock types, each in three fractions, using the µCT SH method. The goal is to develop an approach for quantitatively describing the shape of crushed concrete aggregate fines that will help to assess the effect of different rock types on shape and, eventually, the effect of shape on fresh properties of concrete.

2. MATERIALS AND METHODS

2.1. Materials

Fine aggregate powder materials used for this study were produced from 10 different blasted and crushed rocks with the nominal size range of about 4 mm to 22 mm. The rock types, used for concrete aggregate production, were chosen from 10 different quarries in Norway to represent a wide range of local mineralogy and mechanical properties. This included (Table 1) intrusive and extrusive igneous, metamorphic, and sedimentary rocks that were both mono- and multi-mineralic. Further processing included high rotor speed (70 m/s) VSI crushing to generate fines and static air-classification of the crusher products into three distinct size fractions with approximately the following d_{10} to d_{90} ranges: 4 µm to 25 µm (fine), 20 µm to 60 µm (medium) and 40 µm to 250 µm (coarse) (Table 1). The parameter d_N equals the percentage, by mass, of particles with sizes less than d. The finest powder fraction (4 µm to 25 µm) included all the

particles smaller than 4 µm generated during the crushing, where particle size was defined by the air-classification process. Air classification uses air to classify a product by size and shape. By accelerating air inside a chamber and adding crushed sand or other mineral feed into the chamber, one can use the counteracting gravitational and/or centrifugal forces versus the drag force of the air to create a classification of particles by their combined shape, weight and density [46]. The initial or original material is divided into two products: coarse and fine. Classification is characterized by a particle cut-size, which is the border between these fractions [47]. Due to various stochastic factors (air turbulence, particle collisions, variations in feed moisture, etc.), some fines get into the coarse product and vice versa [47]. Over recent decades a number of air classifiers have been developed and a comprehensive overview of different types of air classification equipment is provided in [47]. In total, 30 different fine powder samples were produced (Table 1): three particle size ranges for each of the 10 rock types. Mineralogical composition of the powders was determined by quantitative X-ray diffraction (XRD) analysis of the 4 µm to 25 µm size fractions (
Table 2) [48].

The VSI crushing and air-classification experiments are described more fully in [10].The experiments were performed under controlled conditions at full scale test facilities and are thus representative of the processes from real production facilities. The air classification consisted of three consecutive classification steps of initial ≤ 2 mm feed materials. Detailed studies of the particle size distribution (PSD) and specific surface area of all the crushed fines were presented in [48].

Table 1: Crushed rock fines used for the study.

Table 2: Mineralogical composition of rock types T1-T10 determined with quantitative XRD [48].

2.2. X-ray µCT combined with spherical harmonic analysis (3-D method)

Combining X-ray µCT with spherical harmonic (SH) analysis for particle size and shape measurements was introduced in [34], [35], [36], [37], [38], [39], [40], [41], [42], [43], [44], [45] and has been applied to very similar crushed aggregate materials in [45] and [52]. Sample

preparation involved casting samples of the crushed powders in epoxy at about 5 % volume concentration and allowing hardening without segregation. After hardening, the samples were scanned using μCT equipment and complete three-dimensional renderings of the digitized particle size and shape were obtained within the limitation of the voxel size used. Particles down to the volume of 8 x 8 x 8 = 512 voxels were used for the analysis. This lower limit is employed since smaller particles are hard to distinguish from background noise in the μCT-scanning, and not enough of details of the particle geometry can be obtained for these smaller particles. The μCT equipment used was a benchtop scanner (Skyscan* 1172 by Bruker), used for the 20 μm to 60 μm and 40 μm to 250 μm size fractions, and an XRM500 Versa instrument (Carl Zeiss X-ray Microscopy) for the 4 μm to 25 μm size fractions. The image size, pixel size, smallest analysed particle sizes and number of analysed particles are listed in

Table 3. The resulting 3-D image, made by stacking the many 2-D images of the sample, is a gray-scale image that needs to be segmented to produce the final 3-D image. In the segmented 3-D digital image, details below the voxel size have been lost, and it is possible that the volume of the particles in the image could be a little smaller or a little larger than reality, due to the choice of threshold used in the segmentation process. However, for larger particles whose volumes could be easily experimentally measured, this technique did give an accurate value (1 % to 2 % uncertainty) of particle volume [36]. There can be errors in the surface area due to "ringing" effects in the actual SH coefficients themselves, akin to the Gibbs' phenomenon in 2-D Fourier series [53], [54], but these errors for random particles are small. The SH coefficients [34] were generated using the μCT data for each of the analysed particles. Using SH functions, one can compute any geometric quantity of the particle, which can be defined by integrals over the volume or over the surface or any other algorithm using points on the particle surface or within the particle volume, since the SH approach gives an analytical, differentiable mathematical form for the particle surface and volume [34], [53], [54].

To describe an average particle "size" we then used the volume equivalent sphere diameter (VESD), which is the diameter of a sphere with the same volume as a given particle. To give a

* Commercial equipment, instruments, and materials mentioned in this paper are identified in order to foster understanding. Such identification does not imply recommendation or endorsement by the National Institute of Standards and Technology (NIST), nor does it imply that the materials or equipment identified are necessarily the best available for the purpose.

measure of particle shape, the length (L), width (W), and thickness (T) can be defined (ASTM 4791 [55]). L is defined as the longest surface-surface distance on the particle, W is defined similarly, but it must be perpendicular to L, and T is the longest surface-surface distance that is perpendicular to both L and W [36]. These dimensions are in principle different from the 3-D equivalents of the 2-D Feret diameters. The two independent aspect ratios, L/T and L/W, are then an estimate of the average aspect ratio of a particle, since L, W, and T define a rectangular box that just encloses the particle. The mean L/W ratios for different subsamples of the same powder type varied in the range of ± 0.02.

Table 3: µCT and SH analysis – pixel size, smallest analysed particle size, image size and number of analysed particles.

3. RESULTS AND DISCUSSION

3.1. Shape characteristics determined by 3-D µCT scanning and spherical harmonic analysis

Figure 1 illustrates mean L/W ratios for all the different rock types and powder fractions, plotted against the mean VESD of the bins for which they have been determined. Particles larger than 12 µm and 150 µm have not been included in Figure 1a and Figure 1c, respectively, because for some of the ten rock types less than 100 particles were falling in the bins above these sizes, which did not allow a valid result. An important observation from the plots in Figure 1 is that the mean shape characteristics for each rock type are essentially the same over all the separate size bins, within an uncertainty of about 5 %. The results from Figure 1 also show that the relative ranking of the shape of crushed aggregate particles from different rock types seems to be about the same over the particle sizes within a bin range over the full width of the bin considered, for all three size ranges. These two observations were also found to be true in identical plots that used the L/T or the W/T ratios as shape description parameters (not included in the paper). This justifies the usefulness of mean shape parameters, which are a single number representing the whole analysed powder sample over a fairly wide particle size range.

The L/W ratios in Figure 1 also show that the shape of the aggregate particles of different rock types are somewhat more similar for particles bigger than about 15 µm equivalent size (VESD), since there is a lower range of variation for the L/W ratios of different rock types for particles bigger than about 15 µm VESD. It also appears that the particles below about 15 µm in size have slightly higher values of the L/W ratios than do the larger particles. Higher values of L/W means less equidimensional particles. This fact suggests that, as the particle size decreases, it is more difficult to affect shape characteristics by the means of VSI crushing. At small particle sizes, it is possible that shape depends more on mineral grain shape than on the VSI crushing process [30], [28]. The same trend can also be seen from analysing the L/T and W/T ratios of the particles when plotted in the same manner as seen in Figure 1 (not included in the paper).

It can also be seen in Figure 1 that the relative ranking of the particle shapes among the various rock-types is different for the three analysed particle size ranges, *i.e.* 4 µm to 25 µm, 20 µm to 60 µm or 40 µm to 250 µm. For example, the most equidimensional shape, or with L/W value closest to unity, was found for the T6 crushed fines, for all three particle size fractions studied. On the other hand, the least equidimensional shape, or highest mean L/W value, was either T3 or T10, depending on which particle size fraction is considered. Remember that the different particle size fractions were produced by means of air-classification. Air classification can affect the distribution of particle shapes among the three different particle size ranges produced from the same rock type, because the path of movement of a particle in the air-classification chamber is affected also by its shape [47], [56], [57], [58], [59], [60]. As a result, certain shapes of particles can preferentially be enriched in either of the two air classification products at either side of the cut-point. This could then be the reason why particles of the same rock-type that belong to the same size-bin, but are obtained from different nominal size-fractions, have somewhat different mean L/W ratios. See, for example, the size range of 40 µm to 65 µm VESD in Figure 1b and Figure 1c, which is present in both figures, where the mean L/W ratios for particles of the same equivalent size are systematically higher for the finer (20 µm to 60 µm) fractions in Figure 1b. Johansson and Evertsson [58] have performed air-classification experiments with quite similar VSI crushed aggregate powders and also observed that the less spherical particles are more likely to end up with the fine product of the classification. They

explained this by the fact that the drag on the particles, which affect the results of the air-classification, depends on the particle shape.

Figure 1: Mean L/W ratios of the analysed crushed powders, with the x-axis corresponding to the VESD of the median size of a bin. (a) 4 µm to 25 µm size fractions (shown to 12 µm, see text); (b) 20 µm to 60 µm size fractions; (c) 40 µm to 250 µm size fractions (shown to 150 µm, see text).

The relation between the mean 3-D shape parameters (L/T, L/W and W/T) of the different rock types is presented in Figure 2. The data in Figure 2 show that the different shape parameters of the crushed aggregate fractions produced by VSI crushing are mutually related, which is illustrated by the relatively high squared linear correlation coefficients R^2, all greater than 0.9 and most close to 1. This implies that the VSI crushing process similarly affects flatness and elongation, reducing both at the same time, since elongation relates more to the L/W ratio and flatness relates more to the W/T ratio.

Figure 2: Relation between shape parameters L/T, L/W and W/T, as determined by 3-D µCT scanning and SH analysis.

3.2. Form models

Shape classification concepts developed by sedimentary petrologists will be used to better interpret the differences of the VSI crushed fines particle shape. In sedimentary geology the lengths of three orthogonal axes $D_1 \geq D_2 \geq D_3$ have been used to quantify particle shape since 1930 [61]. The triaxial dimensions D_1, D_2, D_3 widely used in the sedimentary geology literature are defined slightly different than the previously defined L, W, T (see section 2.2.2) that are used to characterise aggregate shape in the construction industry [53]. In sedimentary petrology D_1 is defined to be the length of the longest line segment that can be drawn between any two surface points. D_2 is the longest dimension of the maximum projected area of the particle that is also perpendicular to D_1, and D_3 is the longest dimension perpendicular to both D_1 and D_2 [62]. L is defined to be the particle's longest axis and is thus equal to D_1. W is the longest axis perpendicular to L and need not bear any relation to the maximum projected area. D_2 must also

be perpendicular to L, but is constrained to lie in the plane of maximum projected area, so $D_2 \leq$ W. Finally, T is the longest axis that is perpendicular to both L and W. Even though there are slight differences in the definition, it has been demonstrated by Bullard and Garboczi [53] that the triaxial dimensions D_1, D_2, D_3 are essentially identical numerically to the L, W, and T dimensions. Thus only the L, W, T is used for the further discussion as being equivalent to D_1, D_2 and D_3 numerically, and because these parameters have actually been determined for the particles analysed in the paper.

Particle shape analysis usually incorporates three geometrical descriptions: form, roundness, and surface texture. These are in principle distinct and separately definable properties [63]. The three concepts are qualitatively illustrated in Figure 3. While shape may also have different meanings for the same person, the two concepts recognized by Griffiths [64] and Sneed and Folk [65] are maintained in the discussion below. Shape is taken to include roundness (=smoothness) and surface texture, and form is used, following the proposal by Sneed & Folk [65], to approximate the gross overall shape of a particle, and is independent of roundness and surface texture [66].

Figure 3: A particle outline (heavy black solid line) with its component elements of form (light solid red lines, two approximations shown), roundness (dashed blue circles) and texture (dotted black circles) identified [66].

As illustrated in Figure 3, form in this case is defined by the three dimensions of a particle based on ratios between the proportions of the long (L), medium (W), and short (W) axes of the particle, which can be used to define the smallest circumscribing ellipsoid or box. A more spherical form is obtained by a particle with nearly equal particle dimensions, L = W = T. Roundness is a measure of the sharpness of the edges and corners of a particle or the degree to which the contour of a particle fits the curvature of the largest sphere that can be contained within the particle (inscribed sphere). Surface texture can be understood as the topography of the surface of a particle on length scales much smaller than the form dimensions, and it is essentially independent of both form and roundness [66], if it can be defined at much smaller length scales. If the length scales of the form dimensions are close to the length scale of the roughness, then these are no longer independent quantities.

Zingg [67] was the first to propose a classification system for particle form based on the three orthogonal axis (L, W, T). He noted that only two independent ratios can be obtained from these three parameters. The values of these two ratios completely define the form within this model. Based on this observation, he introduced a diagram (Figure 4a) where the flatness ratio p = T/W is plotted against the elongation ratio q = W/L and defined four shape classes on the basis of an arbitrary fixed 2/3 ratio. These shapes are called **I disc**; **II sphere/cubic**; **III blade** (flat and elongated); and **IV rod** (Figure 4a). The II class can be a sphere or a cube, since both are equidimensional under the definition we are using for form. The drawback of the simple system by Zingg [67] is, however, that the obtained particles classes are very wide and not suitable for distinguishing between particles of a comparably similar shape.

Other mathematical interpretations of the form have also been devised. Wadell [68], [69], [66], argued for using the sphere as a reference form (Ψ), and considered that the deviations are best represented by ratios of the particle volume to the volume of the circumscribing sphere:

$$\Psi = \sqrt[3]{\frac{V_p}{V_{cs}}}, \qquad (1)$$

where

V_p = volume of the particles;

V_{cs} = volume of the circumscribing sphere.

Wadell's [68], [69] definition is, however, sensitive to both roundness, as well the form, because rounding the edges of a cube changes Wadell's sphericity, but not its form, as defined by the L/W value [66]. Therefore, it is not equivalent to the form as defined by Zingg [67], but includes some aspect of roundness. The difference between the approaches of Zinng [67] and Wadell [68], [69] for describing particle shape was reduced by Krumbein [62], [66]. He [62], [66] derived an equation (Equation (2)) for estimating Wadell's [68], [69] sphericity from measurements of the three orthogonal axes of a particle. The principal assumption of the derivation was that the rock particle could be approximated by an ellipsoid. Krumbein's definition of sphericity, which he denoted as intercept sphericity, is then the cube root of the

volume ratio of the ellipsoid, defined by three axes equal to L, W, and T, to the volume of the circumscribing sphere, which has diameter equal to L [62], [66]. In contrast to Wadell's [68], [69] interpretation, Krumbein's [62] intercept sphericity is a function of the form only, as has been defined [66].

$$\Psi_I = \sqrt[3]{\frac{W \cdot T}{L^2}} = \left(\frac{L}{W} \cdot \frac{L}{T} \right)^{-1/3}, \quad (2)$$

where

L = length of the particle (greatest orthogonal length);

T = thickness of the particles (intermediate orthogonal length);

W = width of the particle (shortest orthogonal length).

Krumbein [62] also recognized that lines of equal intercept sphericity plot as hyperbolic curves on Zingg's [67] diagram (Figure 4a) [66], but later Aschenbrenner [70], [66] recognized that another parameter was needed to describe variations in the form for particles of equal sphericity. He [70] introduced a shape factor F that had a range of 0 to infinity and that could also be plotted on the Zingg's [67] plot (Figure 4a):

$$F = \frac{L \cdot T}{W^2} = \frac{L/W}{W/T}. \quad (3)$$

If the shape factor F is greater than 1.0, then L/W is greater than W/T, so the shape is more prolate (rod-shaped). If the shape factor is less than 1.0, then L/W is less than W/T, and the shape is more oblate (disc-shaped) [71]. Williams [72] provided a transformation of Aschenbrenner's [70] shape factor to range from +1 to -1.

In addition to the above form descriptions, other parameters have been devised to estimate form from the three orthogonal axes (L, W, T). For example, Barrett [66] has listed 12 and Rodriguez et al. [73] have listed 11 different parameters describing particle form, which have been derived from L, W, and T. The most applicable form description parameter can also be chosen based on

performance based criteria. For example, Hofmann's shape entropy (see Equation (4)) [74] has attracted attention recently for its ability to correlate with particle setting velocity [75], [76].

$$S_H = \frac{1}{\ln(1/3)} \sum_{i=1}^{3} p_i \ln p_i \,, \tag{4}$$

where

$$p_1 = \frac{L}{L+W+T}$$

$$p_2 = \frac{W}{L+W+T}$$

$$p_3 = \frac{T}{L+W+T}$$

However, Mclean [77] has argued that the most widely used method for designating particle form is still the first classification method by Zingg [67], because of its simplicity and ease of use and interpretation.

3.3 Modelling form with µCT SH data

The data from Figure 2 were plotted in Figure 4b Zingg's diagram [67], along with hyperbolic curves of the Krumbein's intercept sphericity [62] and Achenbrenner's shape factor [70]. In addition, mean flatness and elongation ratio data from some previous studies [43], [45], [52] of µCT and SH shape analysis of different types of similar-sized mineral powders have been summarized in

Table 4 and also incorporated in Figure 4b.

Figure 4: Zingg's diagram [67], showing the relationship between the axial ratios W/L and T/W, Krumbein's intercept sphericity Ψ_I [62] and Aschenbrenner's shape factor F [70]; (a) general particle shape classification chart, after [61]; (b) relationship between the mean axial ratios of the particles from this study and mean axial ratios obtained from previous studies on similar-sized mineral particles according to

Table 4. The data in (b) are numbered according to the labelling scheme of

Table 4.

Table 4: Mean axial ratios obtained from some previous studies on similar-sized mineral particles as the VSI crushed powders analysed within the given study.

It can then be seen from Figure 4b, in light of the variability of the data from Table 4, that surprisingly similar mean shape characteristics have been obtained for all the VSI crushed powder particles, no matter the rock type or size fraction. The plots suggest that most of the particles have the Achenbrenner's [70] shape factor F slightly lower than one. In fact a calculation by Equation (3) gives a result in the order of 0.87-1.02, with an average value of 0.95 and only one value exceeding 1.0. This suggests that most of the particles are quite equidimensional and not particularly prolate or oblate. Figure 4b also shows that the difference in terms of the mean sphericity of the different crushed powder particle samples is not great. Expressed in numbers, the Krumbein's intercept sphericity [62], according to Equation (2), varies over the range of 0.66 to 0.75. The data in Table 4 (and the additional corresponding data points in Figure 4b) includes fines from some similar rock types and other mineral materials produced with other comminution methods, *e.g.* milling and cone crushing. These results show that most of the shapes obtained are clearly less equidimensional than the 30 tested samples of the fines produced during the VSI crushing.

The above observation from Figure 4 concerning the relatively high degree of shape similarities of the 30 different particle types is somewhat surprising because 10 different rock types included in the study have significantly different mineralogical composition (
Table 2), with very different rock texture anticipated. It can also be seen from Figure 1 that for the finest and medium analysed particle size ranges (Figure 1a and Figure 1b), the rock type T10, with the highest content of mica (see
Table 2), had the least equidimensional shape. This to some extent supports the previous observation by Åkesson and Tjell [28], who suggested that it is in general impossible to improve the shape of single mica grains with VSI crushing. The most equidimensional shape in the studied particle size range was found for the two analysed limestone rock types, T5 and T6.

3.4 Micro Flakiness Index (µFI)

Flakiness Index (FI) is the shape parameter that is most often measured for describing crushed rock particle shape in routine quality control in the concrete and aggregate industries [73], [80]. The value of FI is determined by sieving the particles through a special type of sieves with rectangular ("bar-sized") sieve openings. The method has only been standardised (EN 933-3 [81]) for particles coarser than 4 mm, even though it has been reported to be successfully applied for particles down to 1.25 mm in size by using a set of custom sized bar-sieves [15]. However, the method is not suitable for finer materials. This is due to difficulties inducing the finer materials to pass through the slots of the bar sieves, which is also due to the great amount of particles in relation to the area of the sieve compared to when analysing coarser particles [82]. The FI value of the particles in the size range of 1.25 mm to 32 mm (typical maximum aggregate size for ready-mix concrete production purposes) is determined on the aggregate fractions denoted d_i/D_i, where d_i is the lower size bound of the range and D_i is the upper one, defined by the openings of square mesh sieves (Table 5). Each size fraction d_i/D_i is then screened through a bar sieve with a bar width opening of $D_i/2$ and a length that is much larger than any possible particle.

The flakiness index for a tested aggregate fraction is calculated as the mass (M_1) of particles with at least one dimension less than $D_i/2$ (*i.e.* particles passing the bar sieve), summed over all sieves used and expressed as a percentage of the total dry mass of the tested particles (M_2):

$$FI = \frac{M_1}{M_2} \cdot 100\% . \qquad (5)$$

Table 5: Sieves used for flakiness index (FI) determination of concrete aggregate particles larger than 1.25 mm.

The most obvious drawback of the FI parameter is its inability to distinguish between disc-like particles (flat) and blade-like particles (flat and elongated) (see Figure 4a, classes I and III) that belong to the same d_i/D_i size group. This is because the slot length will always be much larger than the length of a particle when a particle is passing through. As a result, both flat and flat and

elongated particles will both be ranked simply as flaky because both will fit through the slot sieves. To see this more clearly, choose a sieve range of d_i and $D_i = 1.25 \cdot d_i$ ($d_i/D_i = 0.8$). Suppose one has two rectangular parallelepipeds, both with $W = 1.2 \cdot d_i$ and $T = 0.6 \cdot d_i$, and one has L = 1.1 W and the other has L = 2 W. Both particles fall into the chosen sieve range, since $d_i < W < D_i$ (1.25 d_i). Both particles would pass through the bar sieve, since $0.6\ d_i < 0.5 \cdot D_i = 0.625 \cdot d_i$. The particle with L/W = 1.1 would be classified as flat, while the particle with L/W = 2 would be both flat and elongated.

There exist other industrial test methods that allow for separate determination of the amount of flat and elongated particles, such as EN 933-4 [83] and ASTM D4791–10 [55], which are performed by using manual proportional calliper devices. However, these methods are only defined for particles larger than 8 mm or 9.5 mm, respectively, and the manual measurements required are tiresome, which prohibits their use on a daily basis for quality control of aggregates. Due to the fast, easy and cheap measurement of a considerable number of particles, FI remains the most popular method for concrete aggregate shape characterisation. Perhaps the reason for the wide acceptance of the test is an indication that the degree of elongation is relatively similar for most concrete aggregate particles that are used for practical applications. If the degree of elongation differed greatly among commonly-used concrete aggregates, which would not affect the FI value, the FI value would not have proven to be useful to practitioners.

The possibility of using the FI value as a single parameter for describing the impact of the shape of coarser concrete aggregate particles (2 mm to 8 mm) on rheological properties of fresh concrete mixes has been investigated in a recent study by Cepuritis et al. [23]. It was demonstrated that changing the FI value of different aggregate particles by 3 % to 50 %, in the particle size fractions 2/5 mm and 5/8 mm, for concrete aggregate from actual production plants, was linearly related to the slump-flow values of a series of concrete mixes when the FI value of one size fraction was varied at a time. The investigated concrete mixes had a water to cement ratio value equal to 0.44, a maximum aggregate size of 8 mm and cement paste matrix content of 438 l/m^3. The cement paste matrix is defined as all fluids, such as water and liquid admixtures, and all particles with size ≤ 0.125 mm, which includes cement and fine mineral filler particles, following the approach in [84], [85]. It was noted that the impact of the FI value increased as the

particle size decreased. The general correlation relationship [23] indicated that an increase in the FI value of the aggregate by 1 % resulted in the reduction of the slump-flow value by 1.9 mm and 2.4 mm for 2/5 mm and 5/8 mm fractions, respectively.

It is nevertheless interesting to compare the particle shape rankings on the micro-scale, as determined for the crushed filler particles by the µCT and SH, to the typical shape variation on the macro-scale for crushed sand and stone aggregate particles. As discussed above, the shape of the latter is most frequently described with the FI parameter. Thus in order to come up with a comparable shape factor for the analysed filler particles, a computational micro-flakiness index (µFI) definition is proposed. This includes extending the series of the standardised d_i/D_i fractions for determination of the FI (Table 5) [81] down to the micrometer-scale size suitable for analysing crushed aggregate powder particles. The principle of such an extension is provided in

Table 6 where sieves down to 2.54 µm are included, as applicable for particles of the current study. However, the extension could be continued to obtain sieve sizes for even smaller particles, as needed. This sieve set, according to

Table 6, was used to define a computational µFI index test by following the same principles as defined in [81]. The first step includes using W from the µCT and SH analysis results for computational particle sieving in order to decide which particles belong to the square opening sieve mass fractions d_i/D_i ($d_i < W < D_i$). This is justified because particle width (W) is the critical dimension in sieve analysis, since all particles in a size range need to have a width smaller than the maximum opening of the largest sieve through which they pass [86]. This is because two of the dimensions for a particle must be smaller than the diagonal width of the square sieve opening in order for the particle to pass through. If W of the particle fits through the sieve, then the T will as well, since by definition it is smaller than the W and is orthogonal to it. L can still be larger than both W and T [40]. Using W as a size parameter from CT and SH analysis of both natural and crushed aggregates from 2.36 mm to 38 mm has shown a good overall relation to traditional sieving results [87]. The second step of the computational µFI test is analysing the obtained d_i/D_i fractions by using the T parameter to decide if the particle can fit through the slot (D_i) of the corresponding bar sieve (

Table 6). L of the particle is assumed to be parallel to the sieve bar. Finally the micro-flakiness index (µFI) is calculated according to Equation (5).

Table 6: index (µFI) determination of concrete aggregate particles down to 2.54 µm in size. The d_i/D_i ratio is set to be always equal to 0.8.

Results of the computational µFI determination were also used to investigate whether it was possible to find a simpler definition of flaky, based only on the particle form measurements (L, W, T), that would map to that defined by the more complicated sieve-bar analysis [81]. This would render the results obtained under the FI definition more directly comparable to the other test methods, *e.g.* ASTM D4791–10 [55] and classification systems, *e.g.* the system by Zingg [67] because of using the same particle geometry parameters. A more computationally simple description of flaky particles that is based on their W and T values is the flatness ratio p = T/W proposed by Zingg [67]. According to Zingg's [67] arbitrary interpretation, if $T \leq p \cdot W$, a particle is classified as flaky for $p < 2/3$ (see Figure 4a). It was then attempted to find such a value of p so that this simpler definition would match the µFI definition down-scaled from the original FI definition of EN 933-4 [81]. It was numerically found that using p = 0.564 provides the best fit for all the analysed 30 powder samples. This is illustrated in Figure 5 where the µFI values obtained by the computation sieving and by the simple definition of $T \leq 0.564 \cdot W$ are related to each other. The good agreement is illustrated by the relatively high squared linear correlation coefficient of $R^2 = 0.98$. Even though the value of p = 0.564 gives results that agree closely with the µFI results(Figure 5), a detailed analysis of which particles of a particular sample are classified as flaky, according to both approaches, reveals that there are a significant number of particles that are classified differently between the two definitions. Thus the closely agreeing flakiness indices (Figure 5) are based on a somewhat different subset of particles. Still, the simple definition is more clear theoretically, as it looks at the actual geometry of given particles where each flaky particle is similar in some way and not on the particle classes of the µFI definition derived from EN 933-3 [81]. The fitted value of p = 0.564 also suggests that the definition of flaky particles by Zingg [67] should actually yield more particles classified as flaky when compared to the definition of the FI from EN 933-3 [81]. This is because Zingg [67] had defined that all particles with $p < 2/3 \approx 0.66$ are classified as flaky, not $p < 0.564$. The definition

of flaky particles from ASTM D4791–10 [55] ($T \leq 0.5 \cdot W$) should then yield the least amount of particles classified as flaky, in comparison to EN 933-3 [81] ($T \leq 0.564 \cdot W$) and Zingg's diagram [67] ($T \leq 0.66 \cdot W$). This is because some particles will pass the criterion of $T \leq 0.564 \cdot W$ and $T \leq 0.66 \cdot W$, butwill not pass the criterion from ASTM D4791–10 [55] of $T \leq 0.5 \cdot W$.

Figure 5: Correlation between the computational µFI following the principles of [81] and the simple definition of $T \leq 0.564 \cdot W$ (all 30 samples, same size ranges and number of particles as in Figure 1).

Results of the computational µFI measurements have been compiled in Figure 6. They indicate a relatively large variation of shapes, if the µFI concept is used to interpret the µCT and SH data. From practical experience of concrete aggregate production, a good quality coarse (particle size ≥ 4 mm to 8 mm) crushed aggregate is expected to have a FI on the order of 10 % to 15 %. Using coarse aggregate with a FI value higher than 35 % is sometimes prohibited [88]. A typical FI value for particles with size less than 8 mm, obtained from Norwegian natural sand and gravel sources, is on the order of 2% to 3 % [9], while an FI value of about 5 % to 8 % is typical for high quality crushed sand production among Norwegian aggregate producers. In fact, analysis of shape in terms of the FI value for aggregate particles from 1.25 mm to 25 mm in size, produced during VSI crushing of the same feed material used to generate the crushed powders studied in this paper, indicated flakiness indices lower than 8 % for all of the rock-types in the analysed size range (Figure 7) [10]. It can then be seen from a comparison of Figure 6 and Figure 7 that if the analysed crushed fines were of a coarse aggregate size their equidimensionality would be evaluated as relatively poor and some might even get rejected, if the same evaluation principles as for coarse aggregates [88] were applied. It can also be concluded that while there exists a clear indication that VSI crushing is able to influence and improve the equidimensionality of small filler particles (Figure 4b) the improvement is considerably smaller than that observed for particles larger than about 1 mm in size, as seen by comparing Figure 6 and Figure 7. We investigated whether the flakiness index shape characteristics obtained for the 1.25 mm to 25 mm particles (Figure 7) related to the shape of the particles of the same rock type but in the 3 µm to 250 µm size range (Figure 6). However, no simple linear, power, logarithmic or exponential relation was found, indicating that formation of particle shape during VSI crushing is governed

by different factors for the particles larger than 1 mm and those in the filler particle range below 250 µm.

Figure 6: Micro-flakiness (µFI) indices of the crushed fine particle fractions after the VSI crushing experiments.

Figure 7: Flakiness index (FI) of the coarse product rock materials after the VSI crushing experiments to generate the analysed crushed fines [10].

4. CONCLUSIONS

VSI crushing is able to generate crushed concrete aggregate fines of similar equidimensional mean shape characteristics down to a particle size of about 3 µm, independent of the very different mineralogical composition of the 10 rock types included in this study. The equidimensionality of the fines generated during the VSI crushing seems to be very consistent and greater than for fines from some similar rock types and other mineral materials produced with other comminution methods, *e.g.* milling and cone crushing. This indicates that it is, indeed, possible to produce crushed sand fines with improved shape characteristics, where improvement means to make more equi-dimensional in comparison to fines produced during other industrial comminution processes. The practical implication of this is that the aggregate producers can expect that VSI crushing will not only increase the equidimensionality of the coarser crushed sand grains, but also generate fines of a favourable particle shape for concrete production for most mineralogical compositions of the feed rock material.

Three size fractions of fines for each of the 10 rocks were analysed. The shape improvement was less effective for particles smaller than about 15 µm, where influence of the crystallographic structure of the individual mineral seems to be more influential. Filler particles of the rock type containing the highest mica content indicated the least equidimensional shape, supporting that mica contributes to irregular shape of fines. It must, however, also be noted that none of the studied rock types was exceptionally rich in mica minerals. The highest mica contents measured for the T8 and T10 rock types were 5.2 mass % and 5.5 mass %, accordingly (see Table 2). From practical experience, this number can also reach up to 30 mass % in some extreme cases, so

aggregate producers shall expect that this could render the average shape characteristics considerably less equidimensional than observed in the given study. The most equidimensional shape among the studied particle size range was found for both limestone rock types studied.

Rather similar particle forms in terms of the classification system typically used by sedimentary petrologists (Zingg's diagram [67]) were found for all the VSI crushed particles analysed. The variation of the particle form was relatively higher if a shape classification parameter used within the concrete industry for coarse particles, the flakiness index (FI), was instead used. An equivalent parameter for the fines was developed: the computational micro-flakiness index (µFI), which is quite similar to the FI but defined for smaller particles and is only accessible computationally when a 3-D characterization of the particle shape is available. In this paper, the 3-D particle shape characterization was carried out via X-ray µCT and spherical harmonic mathematical analysis. The µFI values indicated that VSI crushing seems to affect the equidimensionality of particles coarser than 1 mm [10] much more than for the filler particles smaller than 250 µm as analysed in this study.

For a given sample of VSI crushed aggregate fines, of the same rock type, uniform particle form characteristics, in terms of particle aspect ratios, were found for the entire size range of 3 µm to 250 µm. This means that from a practical concrete proportioning point of view, it may be possible to find mean shape description parameters that can model the influence of the particle shape of the whole sample on the rheological properties of filler modified cement paste and concrete.

5. FUTURE WORK

Further work will involve applying the 3-D µCT and SH method for the detailed analysis of the particle shape of crushed fines produced from the rock types used in this study as a result of blasting and cone crushing. A rock type of higher mica content (preferably up to some 30 mass %) than the rock types studied herein should also be used to generate fines with different comminution techniques (including VSI crusher) to better understand the effect of this sheet

mineral. This should enable an even better understanding of the effect of the VSI crushing on improving the equidimensionality of aggregate particles down to the equivalent size of about 3 µm. The VSI crushed aggregate fines produced for the research reported in this paper will further be used in studies to foster understanding on the influence of their shape and mineralogy on the rheological properties of fresh filler modified cement pastes.

ACKNOWLEDGEMENTS

This work is based on work performed in COIN – Concrete Innovation Centre (www.coinweb.no) – which is a Centre for Research based Innovation, initiated by the Research Council of Norway (RCN) in 2006. The authors would like to gratefully acknowledge COIN for financial support and for facilitating the interaction between research and industry. The authors would also like to acknowledge Dr. Kenneth Snyder, the Acting Deputy Division Chief and Leader of the Inorganic Materials Group at the National Institute of Science and Technology (NIST), for facilitating the collaboration between the Norwegian University of Science and Technology and NIST. The help of lab engineer Steinar Seehuus with the preparation of the epoxy embedded specimens for µCT scanning is greatly appreciated.

REFERENCES

[1] E. Hämäläinen, «Manufactures sand success with Velde Pukk in Norway.,» *Metso's customer magazine for the mining and construction industries - results: minerals&aggregates*, vol. 2, pp. 6-7, 2010.

[2] D. Morrow, «Why manufactured sand?,» *Metso's customer magazine for the mining and construction industries - results: minerals&aggregates*, vol. 1, pp. 26-27, 2011.

[3] R. Cepuritis, «New type of crushed sand to replace natural sand in concrete production.,» *Metso's customer magazine for the mining and construction industries - results: minerals&aggregates*, vol. 2, pp. 38-43, 2014.

[4] H. Pettingel, «An effective dry sand manufacturing process from Japan. Potential to replace natural sand entirely in concrete,» *Quarry Management Magazine*, vol. June, pp. 1-6, 2008.

[5] T. Kaya, «The development of sand manufacture from crushed rock in Japan, using advanced VSI technology. Importance of fine aggregate shape and grading on properties of concrete,» i *Proceedings of 17th Annual Symposium of International Centre for Aggregates Research*, Austin, Texas, 2009.

[6] Robo Silicon, «The Future of Sand is Here,» 2014. [Internett]. Available: http://www.robo.co.in/Download_RoboSand.pdf. [Funnet 09 12 2014].

[7] Sandvik Rock Processing, "Merlin-VSI(TM) setting the standard in VSI crushing," [Online]. Available: http://www.miningandconstruction.sandvik.com/sandvik/9082/Internet/S002630.nsf/Alldocs/Products*5CCrushers*and*screens*5CVSI*impact*crushers*2ARP106/$file/Merlin%20VSI%20ENG.pdf. [Accessed 09 12 2014].

[8] B. Schouenborg, "Resources for Concrete Production," in *Challenges for Sustainable Construction: the "concrete" approach*, Warsaw, Poland, May 18th and 19th, 2006.

[9] R. Cepuritis, "Manufactured sand crushing process parameters: short review and evaluation for sand performance in fresh concrete," *Nordic Concrete Research,* vol. 48, pp. 27-48, 2013.

[10] R. Cepuritis, S. Jacobsen and T. Onnela, "Sand production with VSI crushing and air classification: optimizing fines grading for concrete production with micro-proportioning," *Minerals Engineering,* vol. 78, pp. 1-14, 2015.

[11] M. Bengtsson and C. Evertsson, "Measuring characteristics of aggregate material from vertical shaft impact crushers," *Minerals Engineering*, vol. 19, pp. 1479-1486, 2006.

[12] M. Bengtsson, P. Svedensten and C. Evertsson, "Improving yield and shape in a crushing plant," *Minerals Engineering*, vol. 22, pp. 618-624, 2009.

[13] M. Bengtsson and C. Evertsson, "Modelling of output and power consumption in vertical shaft impact crushers," *International Journal of Mineral Processing*, vol. 88, pp. 18-23, 2008.

[14] M. Ramos, M. Smith and T. Kojovic, "Aggregate shape: prediction and control during crushing," *Quarry Management,* no. November, pp. 23-30, 1994.

[15] R. Cepuritis, "Effects of Concrete Aggregate Crushing on Rheological Properties of Concrete and Matrix. Master thesis," Norwegian Univeristy of Science and Technology, 2011.

[16] R. Cepuritis, "Building on Sand," *International Cement Review,* no. December, pp. 81-83, 2014.

[17] R. Cepuritis, "From Stockpile to Sand," *Quarry,* no. July, pp. 22-28, 2014.

[18] R. Cepuritis, "Sand from the Rocks. New type of crushed sand to replace natural sand in concrete production," *Bulk Solids Handling*, vol. 3, pp. 42-48, 2014.

[19] N. Ahn, "An experimental study on the guidelines for using higher contents of aggregate micro fines in Portland cement concrete. PhD," The University of Texas, 2000.

[20] P. Quiroga, "The effect of the aggregate characteristics on the performance of Portland cement concrete," The University of Texas, 2003.

[21] M. Westerholm, B. Lagerblad, J. Silwferbrand and E. Forssberg, "Influence of fine aggregate characteristic on the rheological properties of mortars," *Cement and Concrete Composites,* vol. 30, no. 4, pp. 274-282, 2008.

[22] D. Cortes, H.-K. Kim, A. Palomino and J. Santamarina, "Rheological and mechanical properties of mortars prepared with natural and manufactured sands," *Cement and Concrete Research*, pp. 1142-1147, 2008.

[23] R. Cepuritis, S. Jacobsen, B. Pedersen and E. Mørtsell, "Crushed sand in concrete – effect of particle shape in different fractions and filler properties on rheology," *Cement and Concrete Composites,* vol. 71, pp. 26-41, 2016.

[24] E. Koehler and D. Fowler, "Research report ICAR 108-2F. Aggregates in Self-Consolidating Concrete," ICAR, Austin, 2007.

[25] M. H. J. Wills, "How aggregate particle shape influences concrete mixing water requirement and strength," *Journal of Materials,* vol. 2, no. 4, pp. 843-865, 1967.

[26] M. Bengtsson, "Quality-Driven Production of Aggregates in Crushing Plants," Chalmers University of Technology. PhD, 2009.

[27] H. Merkus, Particle Size Measurements: Fundamentals, Practice, Quality., Dordrecht: Springer Netherlands, 2009.

[28] U. Åkesson and B. Tjell, "Geological parameters controlling the improvement of manufactured sand using vertical shaft impact crushers instead of cone crushers," in *XXV International Mineral Processing Congress (IMPC)*, Brisbane, QLD, Australia, 6th to 10th of September, 2010.

[29] G. Lowrison, Crushing and Grinding. The Size Reduction of Solid Materials, London: Butterworths, 1974.

[30] B. Lagerblad, H.-E. Gram and M. Westerholm, "Evaluation of the quality of fine materials and filler from crushed rocks in concrete production," *Construction and Building Materials,* vol. 67, pp. 121-126, 2014.

[31] M. Westerholm and B. Lagerblad, "Filler and filler quality of crushed rocks in concrete production," in *International Conference on Building Materials "18. ibausil"*, Weimar, Germany 12th-15th September., 2012.

[32] K.-J. Loorents, E. Johansson and H. Arvidsson, "Free mica grains in crushed rock aggregates," *Bulletin of Engineering Geology and the Environment,* vol. 66, no. 4, pp. 441-447, 2007.

[33] B. Lagerblad, "Crushed rock as aggregate for concrete. Final report. MinBaS project No. 2.2 Future concrete- Subproject 2.23 Utilization of alternative types of aggregates in concrete. MinBaS area 2. Report 2:19 (In Swedish)," MinBaS, Stockholm, 2005.

[34] E. Garboczi, "Three-dimensional mathematical analysis of particle shape using x-ray tomography and spherical harmonics: application to aggregates used in concrete," *Cement and Concrete Research,* vol. 32, pp. 1621-1638, 2002.

[35] S. Erdoğan, P. Quiroga, D. Fowler, H. Saleh, R. Livingston, E. Garboczi, P. Ketcham, J. Hagedorn and S. Satterfield, "Three-dimensional shape analysis of coarse aggregates: new techniques for and preliminary results on several different coarse aggretates and reference rocks," *Cement and Concrete Research,* vol. 36, pp. 1619-1627, 2006.

[36] M. A. Taylor, E. J. Garboczi, S. T. Erdoğan and D. W. Fowler, "Some properties of irregular 3-D particles," *Powder Technology,* no. 162, pp. 1-15, 2006.

[37] E. Masad, S. Saadeh, T. Al-Rousan, E. Garboczi and D. Little, "Computations of particle surface characteristics using optical and x-ray CT images," *Journal of Computational Materials Science,* vol. 34, pp. 406-424, 2005.

[38] E. Garboczi and J. Bullard, "Shape analysis of a reference cement," *Cement and Concrete Research,* vol. 34, pp. 1933-1937, 2004.

[39] G. Cheok, W. Stone and E. Garboczi, "Using LADAR to characterize the 3D shape of aggregates: preliminary results," *Cement and Concrete Research,* vol. 36, pp. 1072-1075, 2006.

[40] S. T. Erdoğan, E. J. Garboczi and D. W. Fowler, "Shape and size of microfine aggregates: X-ray microcomputed tomography vs. laser diffraction," *Powder Technology,* no. 177, pp. 53-63, 2007.

[41] L. Holzer, R. Flatt, S. Erdoğan, J. Bullard and E. Garboczi, "Shape comparision between 0.4 μm to 2.0 μm and 20 μm to 60 μm cement particles," *Journal of American Concrete Society,* vol. 93, pp. 1626-1633, 2010.

[42] S. Erdoğan, X. Nie, P. Stutzman and E. Garboczi, "Micrometer-scale 3D shape characterization of eight cements: particle shape and cement chemistry, and the effect of particle shape on laser diffraction particle size measurement," *Cement and Concrete Research,* vol. 40, pp. 731-739, 2010.

[43] E. Garboczi, "Three dimensional shape analysis of JSC-1A simulated lunar regolith particles," *Powder Technology,* vol. 207, pp. 96-103, 2011.

[44] E. Garboczi and A. Haleh, "National Cooperative Highway Research Program 20-07 (243): Development of Glass Beads Utilised in Traffic Markings," Transportation Research Board, Washington, 2010.

[45] R. Cepuritis, B. Wigum, E. Garboczi, E. Mørtsell and S. Jacobsen, "Filler from crushed aggregate for concrete: Pore structure, specific surface, particle shape and size distribution," *Cement and Concrete Composites,* vol. 54, pp. 2-16, 2014.

[46] K. Aslaksen Aasly, S. Danielsen, B. Wigum, S.-H. Norman, R. Cepuritis og T. Onnela, «Review report on dry and wet classification of filler materials for concrete. State-of-the-art. COIN Project report 52 – 2014,» SINTEF, Oslo, 2014.

[47] M. Shapiro og V. Galperin, «Air classification of solid particles: a review,» *Chemical Engineering and Processing,* vol. 44, pp. 279-285, 2005.

[48] R. Cepuritis, E. Garboczi, C. Ferraris, F. Jacobsen and B. Sørensen, "Measurement of particle size distribution and specific surface area for crushed concrete aggregate fines," *Manuscript submitted for publication to Cement and Concrete Composites.*

[49] E. Garboczi, X. Liu and M. Taylor, "The 3-D shape of blasted and crushed rocks: From 20 μm to 38 mm," *Powder Technology,* vol. 229, pp. 84-89, 2012.

[50] J. Bullard and E. Garboczi, "Defining shape measures for 3-D star-shaped particles: sphericity, roundness, and dimensions," *Powder Technology,* no. 249, pp. 241-252, 2013.

[51] E. Garboczi and J. Bullard, "Contact function, uniform-thickness shell volume, and convexity measure for 3-D star-shaped particles," *Powder Technology,* no. 237, pp. 191-201, 2013.

[52] American Society for Testing and Materials, "Standard Test Method for Flat Particles, Elongated Particles, or Flat and Elongated particles in Coarse Aggregate," ASTM, Pennsylvania, ASTM D4791-10.

[53] R. Johansson, "Dry Classification of Fine Aggregates for Concrete and Asphalt. Lic. thesis," Chalmers University of Technology, 2011.

[54] R. Johansson and M. Evertsson, "CFD simulation of a gravitational air classifier," *Minerals Engineering,* no. 33, pp. 20-26, 2012.

[55] R. Johansson and M. Evertsson, "CFD simulation of a centrifugal air classifier used in the aggregate industry," *Minerals Engineering,* no. 63, p. 149–156, 2014.

[56] R. Johansson and M. Evertsson, "An empirical study of a gravitational air classifier," *Minerals Engineering,* vol. 31, pp. 10-16, 2012.

[57] K. Aslaksen Aasly, S. Danielsen, B. Wigum, S.-H. Norman, R. Cepuritis and T. Onnela, "Review report on dry and wet classification of filler materials for concrete. State-of-the-art. COIN Project report 52 – 2014," SINTEF, Oslo, 2014.

[58] V. Janoo, "Special Report 98-1. Quantification of Shape, Angularity, and Surface Texture of Base Course Materials," US Army Corps of Engineers - CRREL, Hanover, 1998.

[59] W. Krumbein, "Measurement and geological significance of shape and roundness of

sedimentary particles," *Journal of Sedimentary Petrology,* vol. 11, pp. 64-72, 1941.

[60] M. Ozol, "Chapter 35 Shape, Surface Texture, Surface Area, and Coatings," in *Significance of Tests and Properties of Concrete and Concrete-Making Materials, ASTM STP 169B,* West Conshohocken, PA, ASTM International, 1978, pp. 584-628.

[61] J. Griffiths, Scientific Method in Analysis of Sediments, New York: McGraw-Hill, 1967.

[62] E. Sneed and R. Folk, "Pebbles in the lower Colorado River, Texas, A study in particle morphogenesis," *The Journal of Geology,* vol. 66, pp. 114-150, 1958.

[63] P. Barrett, "The shape of rock particles, a critical review," *Sedimentalogy,* vol. 27, pp. 291-303, 1980.

[64] T. Zingg, "Beitrag zur Schotteranalyse," *Schweiz. Mineralog. und Petrog. Mitt.,* vol. 15, pp. 39-140, 1935.

[65] H. Wadell, "Volume, shape and roundness of rock particles," *The Journal of Geology,* vol. 40, pp. 443-451, 1932.

[66] H. Wadell, "Sphericity and roundness of rock particles," *The Journal of Geology,* vol. 41, pp. 310-331, 1933.

[67] B. Aschenbrenner, "A new method of expressing particle sphericity," *Journal of sedimentary petrology,* vol. 26, pp. 15-31, 1956.

[68] T. Powers, The Properties of Fresh Concrete, New York: John Wiley & Sons, 1968.

[69] E. Williams, "A method of indicating particle shape with one parameter," *Journal of sedimentary petrology,* vol. 35, pp. 993-996, 1965.

[70] J. Rodriguez, T. Edeskä r and S. Knutsson, "Particle Shape Quantities and Measurement Techniques–A Review," *The Electronic Journal of Geotechnical Engineering,* vol. 18, pp. 169-198, 2013.

[71] H. Hofmann, «Comparison of sphericity indices and isometric graphs,» *J. Sediment. Res.,* vol. 64, pp. 916-920, 1994.

[72] J. Le Roux, «Comparison of sphericity indices as related to the hydraulic equivalence of settling grains,» *J. Sed. Petrol.,* vol. 67, nr. 3, pp. 527-530, 1997.

[73] J. Le Roux, «Application of Hofmann shape entropy to determine the settling velocity of irregular, semi-ellipsoidal grains,» *Sediment. Geol.,* vol. 149, pp. 237-243, 2002.

[74] R. Mclean, "Zingg shape," in *Encyclopedia of Earth Science. Beaches and Coastal Geology*, Springer, 1982, p. 885.

[75] L. Uthus and I. a. H. I. Hoff, "Evaluation of grain shape characterization methods for unbound aggregates," in *7th International Conference on the bearing capacity of roads, railways and airfields*, Trondheim, Norway, 2005.

[76] European Committee for Standardization, "EN 933-3:2012 Tests for geometrical properties of aggregates - Part 3: Determination of particle shape - Flakiness index," CEN, Brussels, 2012.

[77] A.-L. Persson, "Image analysis of shape and size of fine aggregates," *Engineering Geology*, vol. 50, p. 177–186, 1998.

[78] European Committee for Standardization, "EN 933-4:2008 Tests for geometrical properties of aggregates. Part 4: Determination of particle shape. Shape index," CEN, Brussels, 2008.

[79] E. Mørtsell, *Modelling the effect of concrete part materials on concrete consistency. PhD*, Norwegian University of Science and Technology (In Norwegian).

[80] E. Mørtsell, M. Maage and S. Smeplass, "A particle-matrix model for prediction of workability of concrete," in *P.J.M. Bartos, Marrs D.L. and Cleland D.J., eds., Proceedings of RILEM conference on production methods and workability of fresh concrete*, London: E&FN Spon.

[81] J. Fernlund, "The effect of particle form on sieve analysis: a test by image analysis," *Engineering Geology*, vol. 50, no. 1-2, p. 111–124, 1998.

[82] S. Erdoğan, "Determination of Aggregate Shape Properties Using X-ray Tomographic Methods and the Effect of Shape on Concrete Rheology. PhD," The University of Texas at Austin, 2005.

[83] Norwegian Public Roads Administration, "Manual R762. Process Code 2. Standard specifications for bridges and quays. Main process 8 (In Norwegian)," Norwegian Public Roads Administration, Oslo, 2012.

[84] American Society for Testing and Materials, "ASTM C33 / C33M - 13 Standard Specification for Concrete Aggregates," ASTM, Pennsylvania, 2013.

[85] European Committee for Standardization, "EN 12620:2008 Aggregates for concrete," CEN, Brussels, 2008.

[86] P. Billberg, "Some rheology aspects of fine mortar part of concrete," KTH Royal Institute of Technology. Lic. thesis, 1999.

VITAE OF THE AUTHORS

Dr. **Rolands Cepuritis** is Post-Doctoral Fellow at Norwegian University of Science and Technology and a project manager at the Norwegian cement producer Norcem. He has ten years of practical experience in fields of aggregate, cement and concrete production, concrete structure contracting and research. He is an author of more than 30 publications related to his fields of experience. He has been awarded Kristaps Morbergs Engineering Scholarship from the University of Latvia in 2008 and European Social Fund Master Student Scholarship in 2010. Dr. Cepuritis is a member of RILEM.

Dr. **Edward J. Garboczi** is a NIST (National Institute of Science and Technology) Fellow in the Applied Chemicals and Materials Division. He has published more than 130 papers. He is a member of the American Physical Society, the American Ceramic Society, the American Concrete Institute (ACI), and RILEM. He received the Robert L'Hermite Medal from RILEM in 1992, the 1992 BFRL Communicator Award, and a Silver Medal from the Department of Commerce in 2009. He is a Fellow of both the American Ceramic Society and ACI and is on the editorial board of Cement and Concrete Research.

Dr. **Stefan Jacobsen** is a professor at Norwegian University of Science and Technology, Department of Structural Engineering where he is teaching M.Sc. level course in Concrete Technology and a PhD level course Concrete: Structure-Property Relationship. Previously he has held a professor position and Narvik College, researcher positions at different research institutes in Norway and worked in the contracting business. He is a member of the ISO TC 71/SC8 Environmental management for concrete and concrete structures, RILEM TC-FPC Formwork pressure, the Norwegian Concrete

Association and the Concrete Innovation Centre. Dr. Jacobsen is author of more than 90 publications.

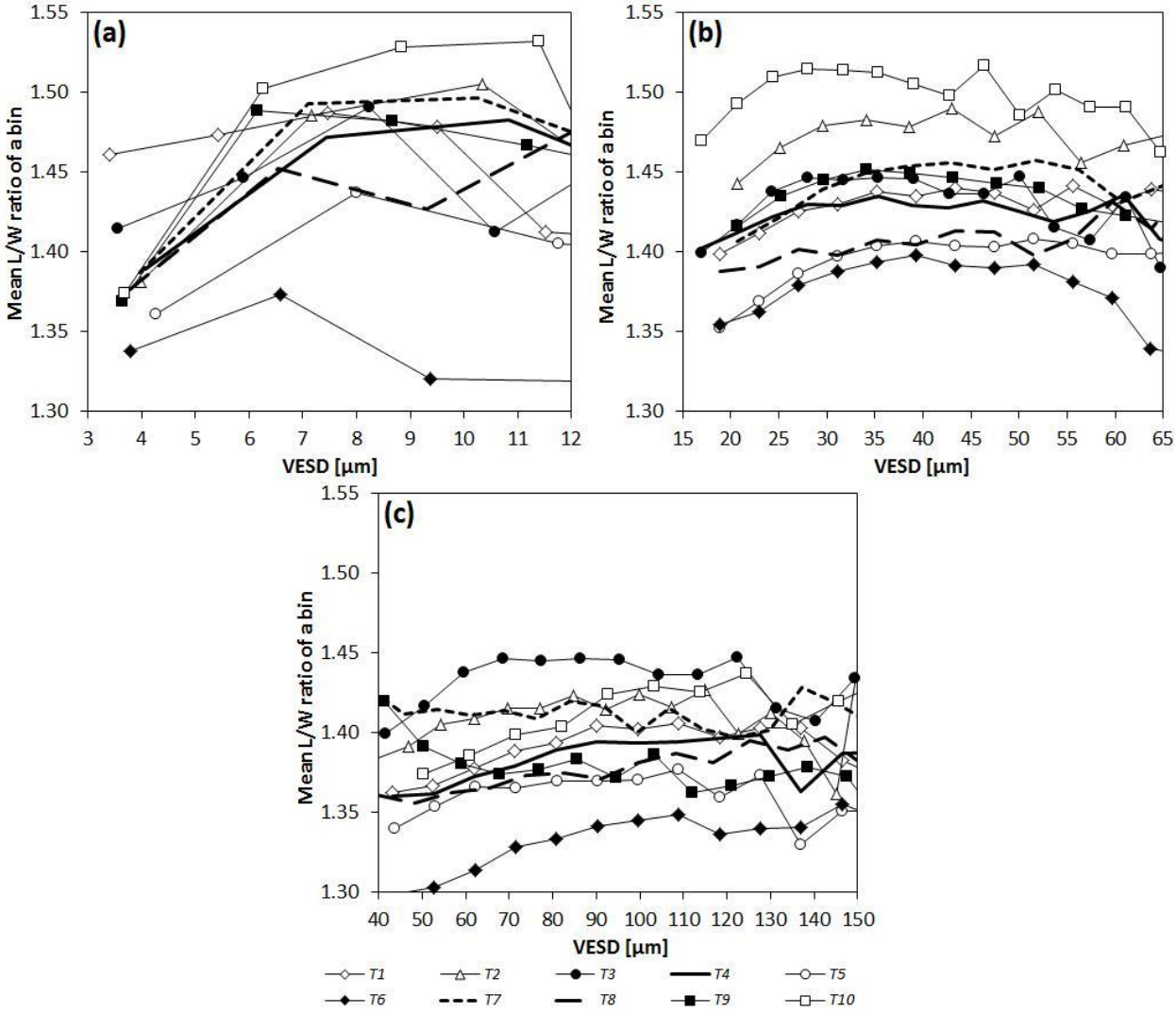

Fig. 1

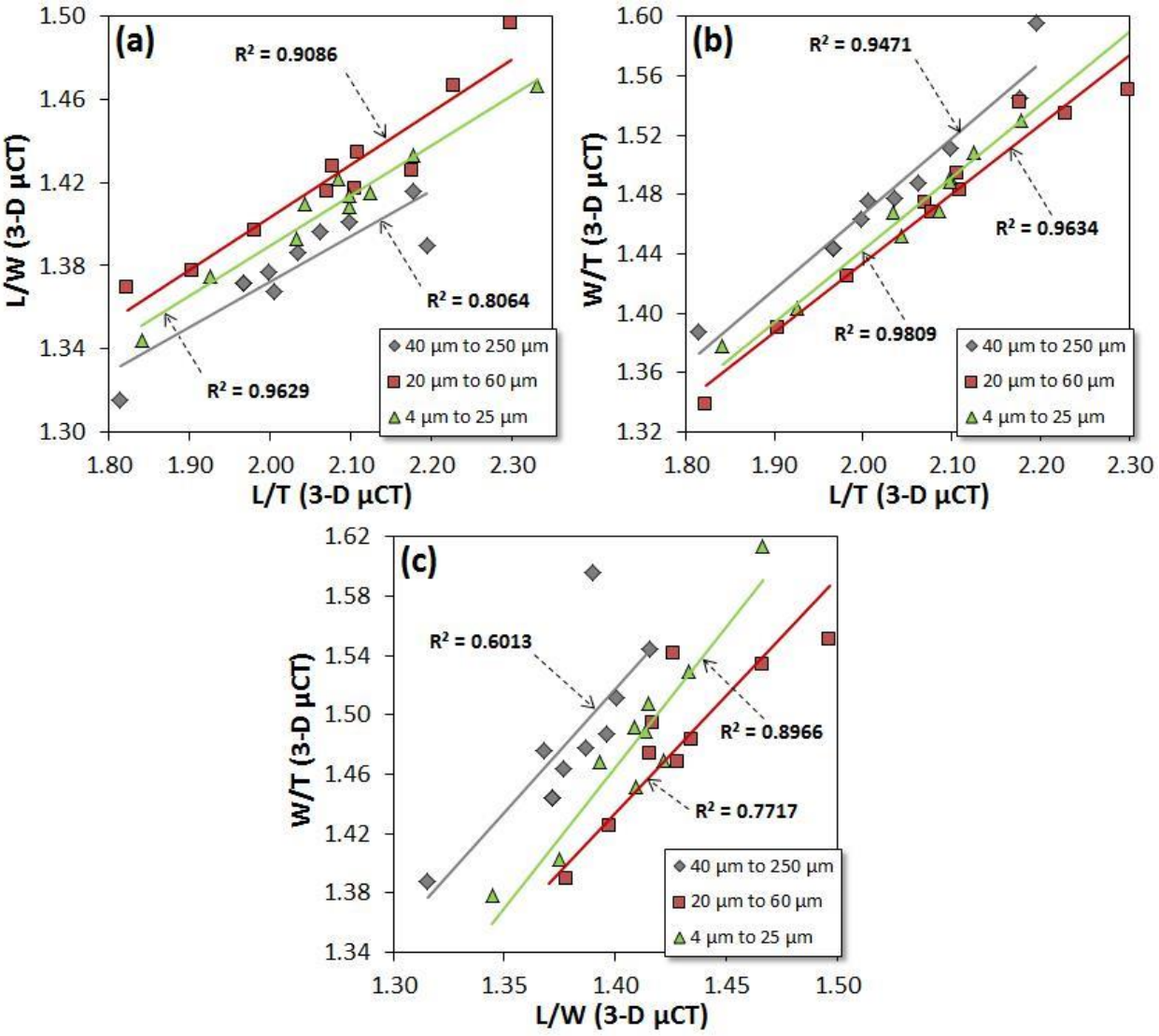

Fig. 2

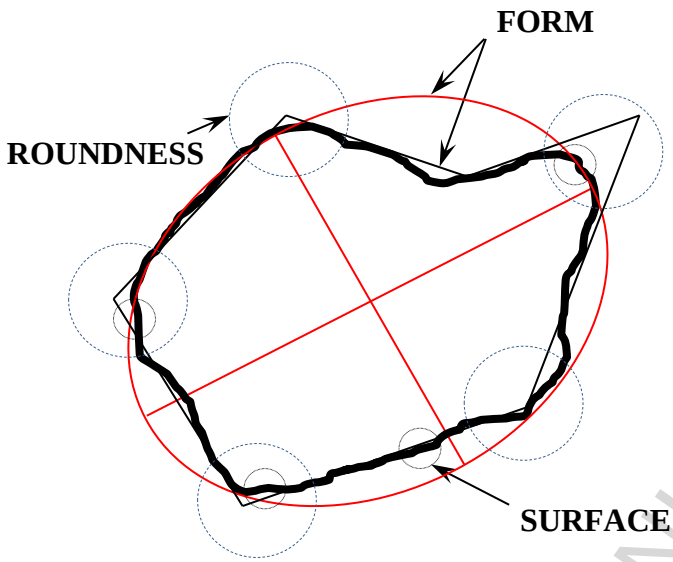

Fig. 3

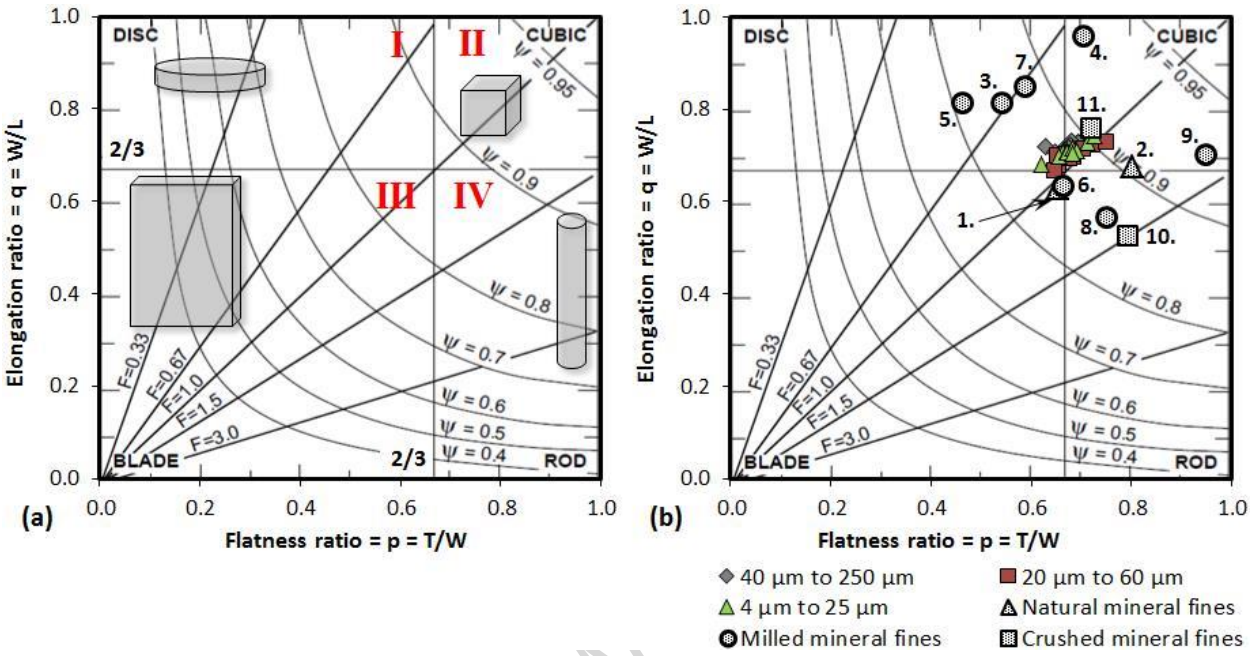

Fig. 4

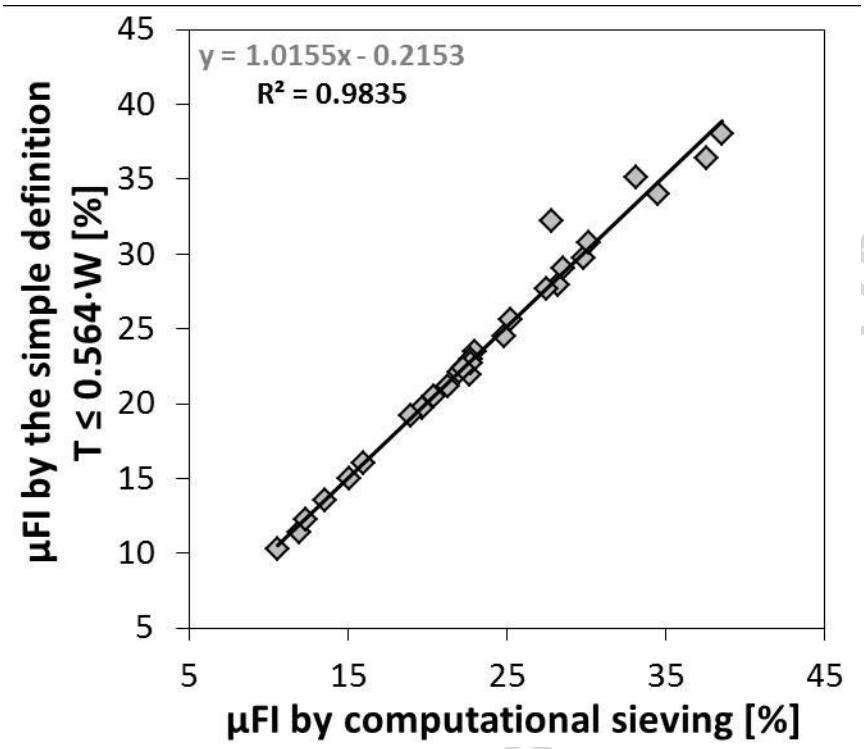

Fig. 5

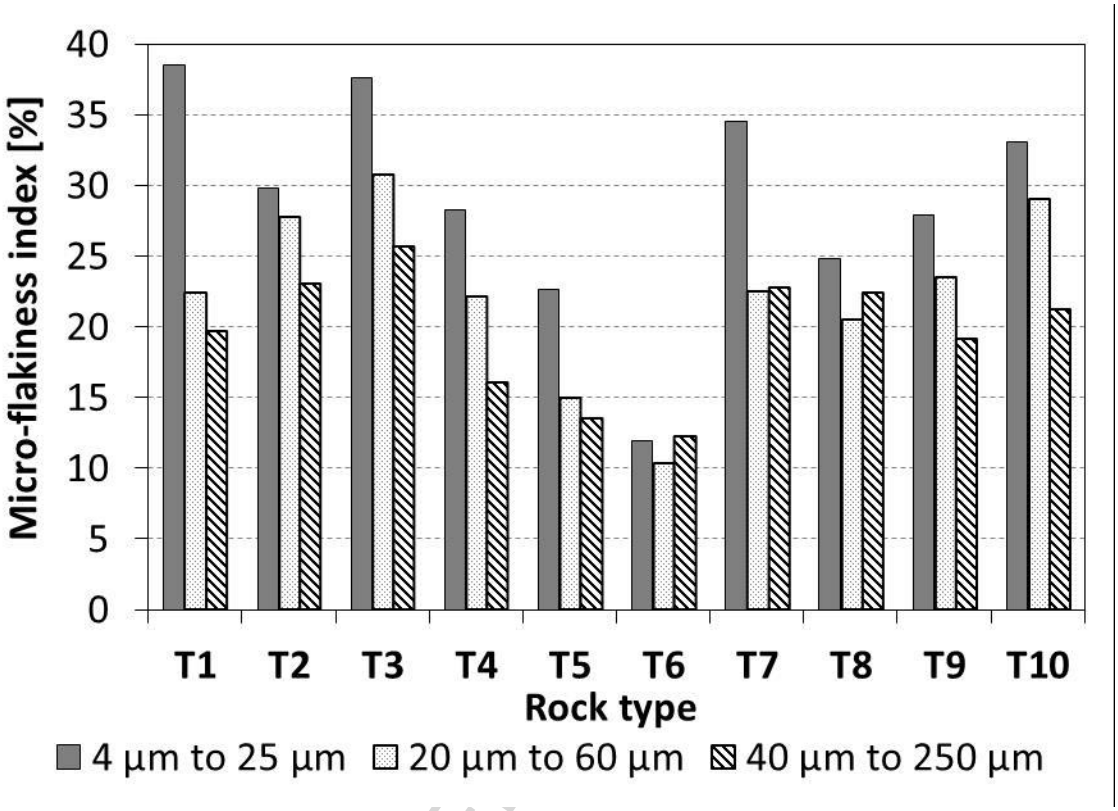

Fig. 6

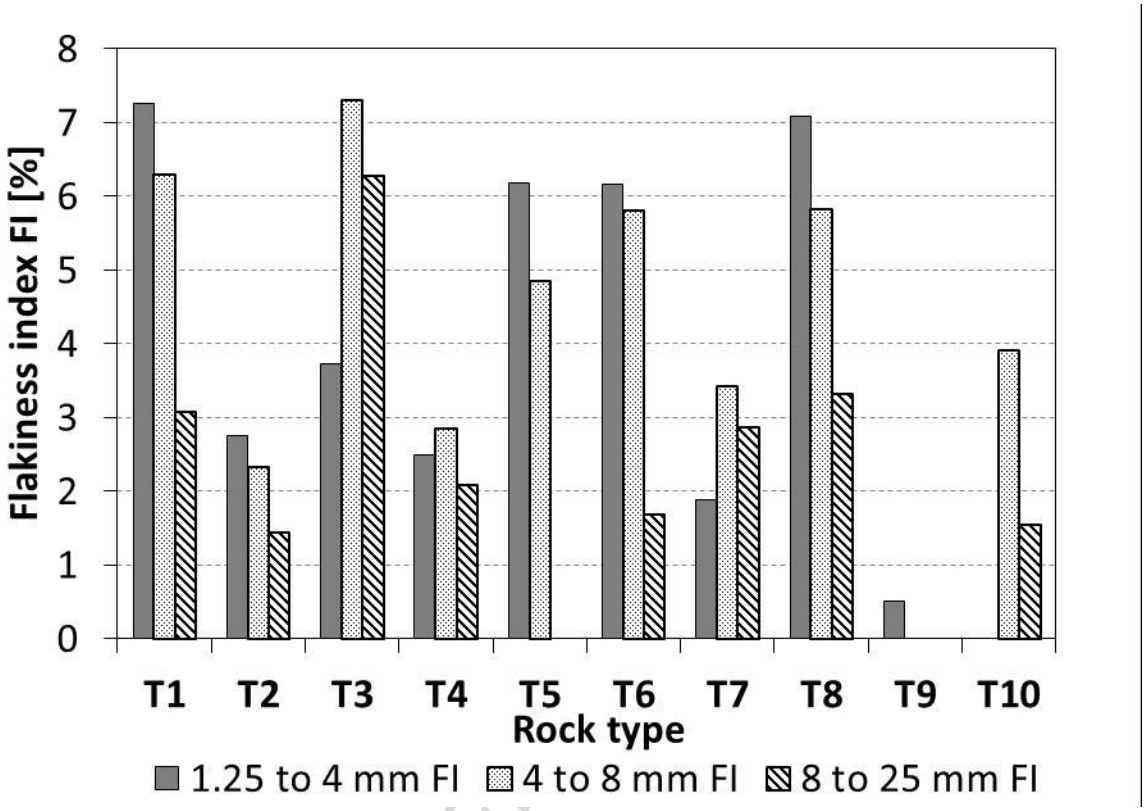

Fig. 7

Table 1: Crushed rock fines used for the study.

Rock type designation	Rock name	Rock type	Mono- or multimineralic	Crushability[a]	Los Angeles value[b]	Crushed rock fines fraction		
						Fine	Medium	Coarse
				[%]	[%]	4 µm to 25 µm	20 µm to 60 µm	40 µm to 250 µm
T1	**Mylonitic quartz diorite**	Metamorphic	Multimineralic	23	12	T1-1	T1-2	T1-3
T2	**Gneiss/ granite**	Metamorphic/ igneous (intrusive)	Multimineralic	41	20	T2-1	T2-2	T2-3
T3	**Quarzite**	Metamorphic	Monomineralic	49	25	T3-1	T3-2	T3-3
T4	**Anorthosite**	Igneous (intrusive)	Multimineralic	28	14	T4-1	T4-2	T4-3
T5	**Limestone**	Sedimentary	Monomineralic[c]	45	22	T5-1	T5-2	T5-3
T6	**Limestone**	Sedimentary	Multimineralic[c]	36	18	T6-1	T6-2	T6-3
T7	**Dolomite**	Sedimentary	Multimineralic	98	92	T7-1	T7-2	T7-3
T8	**Basalt**	Igneous (extrusive)	Multimineralic	18	11	T8-1	T8-2	T8-3
T9	**Aplite**	Igneous (intrusive)	Multimineralic	40	20	T9-1	T9-2	T9-3
T10	**Granite/ gneiss**	Igneous (intrusive)/ metamorphic	Multimineralic	54	29	T10-1	T10-2	T10-3

[a] Determined according to the French standard NF P18-579 (1990) [49], [10] .

[b] The Los Angeles standard values according to EN 1097-2 [50] have been approximated from the crushability testing results using the correlation relationship available in [51].

[c] According to the XRD analysis results (
Table 2) T5 and T6 have 95-97 % carbonate minerals. However, while T5 has 97 % limestone ($CaCO_3$), T6 has 74.5 % limestone ($CaCO_3$) and 20.5 % dolomite minerals ($CaMg(CO_3)_2$) and thus cannot be considered monomineralic.

Table 2: Mineralogical composition of rock types T1-T10 determined with quantitative XRD [48].

Rock type	**Mylonitic quartz diorite**	**Gneiss/ granite**	**Quartzite**	**Anorthosite**	**Limestone**	**Limestone**	**Dolomite**	**Basalt**	**Aplite**	**Granite/ gneiss**
Rock type designation	**T1**	**T2**	**T3**	**T4**	**T5**	**T6**	**T7**	**T8**	**T9**	**T10**
Tested fraction	4 µm to 25 µm									
Mineral or group of minerals	Mass %									
Quartz	27.9	20.9	90.0	6.5	2.3	2.5	1.1	8.9	36.2	17.8
Carbonate minerals	4.4	-	3.6	10.6	97.7	95.0	95.0	8.3	-	5.0
Epidote minerals	8.4	-	-	24.4	-	-	-	7.6	-	-
Feldspar minerals	37.7	63.9	3.9	33.1	-	0.4	0.6	26.5	58.2	58.8
Sheet silicates (micas[a])	1.3	3.7	1.5	-	-	1.1	-	5.2	2.7	5.5
Sheet silicates (other)	6.7	4.4	-	20.4	-	0.4	0.7	0.0	0.0	3.7
Chlorite	11.3	1.4	1.0	2.6	-	0.6	1.6	20.2	1.7	0.5
Inosilicate minerals	1.0	3.9	-	2.3	-	-	1.1	11.0	1.2	8.7
Iron oxide minerals	-	-	-	-	-	-	-	3.5	-	-
Other minerals	1.3	1.9	-	0.2	-	-	-	8.8	-	-

[a] Biotite and muscovite.

Table 3: µCT and SH analysis – pixel size, smallest analysed particle size, image size and number of analysed particles.

Fraction	**4 µm to 25 µm**	**20 µm to 60 µm**	**40 µm to 250 µm**
Average pixel size used for the µCT scanning [µm]	0.32	1.71	3.87
Smallest analysed particle size (VESD of a 512 voxel particle) [µm]	3.18	16.97	38.41
Image size [pixels]	ca. 900 x 968	2000 x 2000	2000 x 2000
Mean number of particles analysed	43 930	1 562 151	953 821

Table 4: Mean axial ratios obtained from some previous studies on similar-sized mineral particles as the VSI crushed powders analysed within the given study.

No in Figure 4b	Mineral material type	Method of final size formation	Analysed particle size range [µm]	Mean flatness ratio p=T/W	Mean elongation ratio q=W/L	Reference with additional data
1	Granite/ gneiss rock	Natural	3/20	0.65	0.63	Cepuritis, et al. [45]
2			20/125	0.80	0.68	
3	Limestone rock	Milling	3/20	0.54	0.81	
4			20/125	0.70	0.96	
5	Slag[b]		10/80	0.46	0.81	n/a[a]
6	Cement[c]		10/100	0.66	0.63	n/a
7	Basaltic volcanic rock (lunar regolith simulant JSC-1A)		20/38	0.59	0.85	Garboczi, et al. [43]
8			38/75	0.75	0.57	
9			155/300	0.95	0.70	
10	Granodiorite rock	Cone crushing	100/200	0.79	0.53	Garboczi, et al. [52]
11			200/635	0.72	0.76	

[a] additional reference is not available; data has been obtained as part of unpublished shape characterization research at National Institute of Standards and Technology (NIST) by one of the authors.

[b] finely ground granulated blast-furnace slag, meets ASTM C 989 [78] specification, from Alabama, US.

[c] portland cement, ASTM Type I, meets ASTM C150 [79] specification, from South Carolina, US.

Table 5: Sieves used for flakiness index (FI) determination of concrete aggregate particles larger than 1.25 mm.

	Regular sieves of square openings			Corresponding bar-sieve (slot size)
	Lower aperture size, d_i	Upper aperture size, D_i	d_i/D_i	$D_i/2$
	[mm]	[mm]	[1]	[mm]
Standard set of sieve combinations according to [81]	31.5	40	0.79	20
	25	31.5	0.79	15.75
	20	25	0.80	12.5
	16	20	0.80	10
	12.5	16	0.78	8
	10	12.5	0.80	6.25
	8	10	0.80	5
	6.3	8	0.79	4
	5	6.3	0.79	3.15
	4	5	0.80	2.5
Custom set of sieve combinations used by Cepuritis [15]	3.15	4	0.79	2
	2	2.5	0.80	1.25
	1.6	2	0.80	1
	1.25	1.6	0.78	0.8

Table 6: index (µFI) determination of concrete aggregate particles down to 2.54 µm in size. The d_i/D_i ratio is set to be always equal to 0.8.

Virtual sieves of square openings			Corresponding virtual bar-sieve (slot size)
Lower aperture size, d_i	Upper aperture size, D_i	d_i/D_i	$D_i/2$
[µm]	[µm]	[1]	[µm]
4000.00	5000.00	0.8	2500.0
3200.00	4000.00	0.8	2000.0
2560.00	3200.00	0.8	1600.0
…	…	…	…
1638.40	2048.00	0.8	1024.0
1310.72	1638.40	0.8	819.2
1048.58	1310.72	0.8	655.4
…	…	…	….
90.07	112.59	0.8	56.3
72.06	90.07	0.8	45.0
57.65	72.06	0.8	36.0
…	…	…	…
7.74	9.67	0.8	4.8
6.19	7.74	0.8	3.9
4.95	6.19	0.8	3.1
…	…	…	…
3.96	4.95	0.8	2.5
3.17	3.96	0.8	2.0
2.54	3.17	0.8	1.6

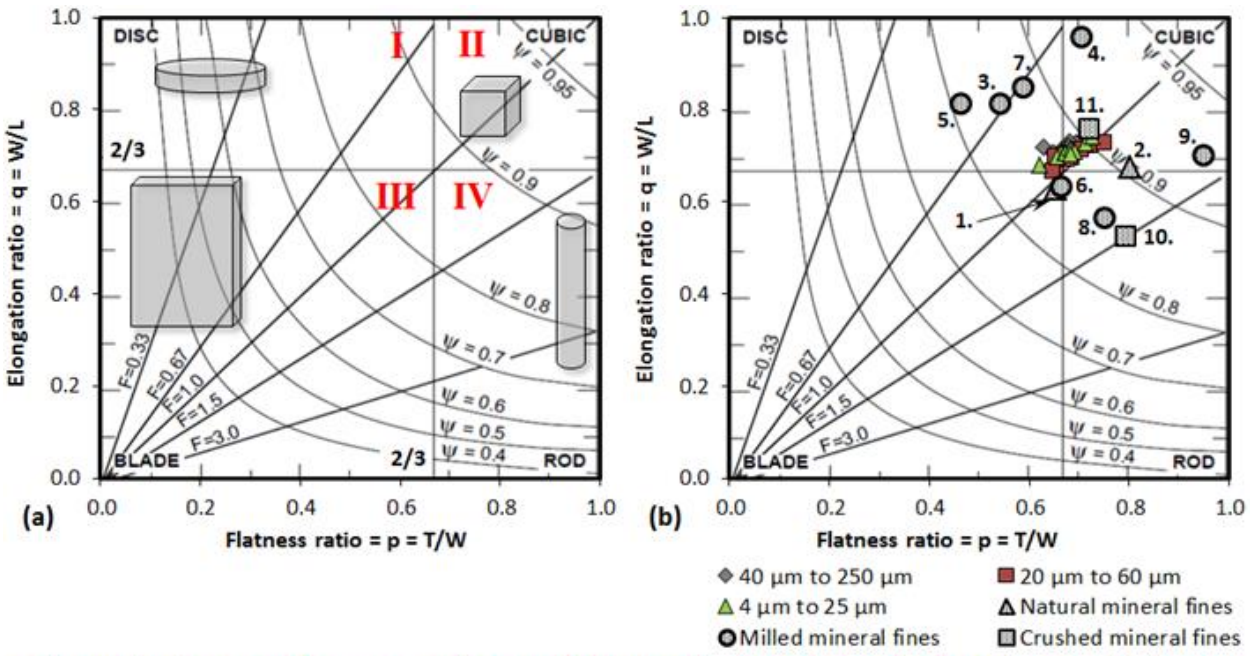

Relationship between the mean axial ratios of the particles from the study plotted in Zingg's diagram

Graphical abstract

Highlights:

- X-ray µCT & spherical harmonics can be applied for particles down to 3 µm in size.
- VSI affects the shape of crushed fines in the size range of 3 µm to 250 µm.
- For particles ≤ 15 µm rock mineralogy is affecting the impact from VSI.
- Micro-Flakiness Index (µFI) is a new parameter for shape of crushed fine particles.